

Petr Knobloch

**On the choice of the  
SUPG parameter at  
outflow boundary layers**

Preprint No. MATH-knm-2007/3

4. 7. 2007

Submitted to *Advances in Computational Mathematics*

---

Department of Numerical Mathematics, Faculty of Mathematics and Physics,  
Charles University, Sokolovská 83, 186 75 Praha 8, Czech Republic

<http://www.karlin.mff.cuni.cz/ms-preprints/>

Cover print by ReproStředisko, Malostranské nám. 25, Praha 1 - Malá Strana

Design by Mirko Rokyta, picture of snowflake by Ondřej Kalenda

Current series administrator: Vít Dolejší

# On the choice of the SUPG parameter at outflow boundary layers

Petr Knobloch

*Charles University, Faculty of Mathematics and Physics, Department of  
Numerical Mathematics, Sokolovská 83, 186 75 Praha 8, Czech Republic*

---

## Abstract

We consider the SUPG finite element method for two-dimensional steady scalar convection–diffusion equations and propose a new definition of the SUPG stabilization parameter along outflow Dirichlet boundaries. Numerical results demonstrate a significant improvement of the accuracy and show that, in some cases, even nodally exact solutions are obtained.

*Key words:* Convection–diffusion equations, Streamline upwind/Petrov–Galerkin (SUPG) method, Spurious oscillations, Outflow boundary layers

---

## 1 Introduction

In many applications, transport processes are the main mechanism determining distributions of the observed physical quantities. Often, the distributions of some of the quantities are not smooth and contain narrow regions where the quantities change abruptly. Depending on the application, one speaks about layers, shocks or discontinuities. When approximating such quantities numerically, the width of the regions where shocks or layers occur is often much smaller than the resolution of the used mesh. Consequently, the shocks or layers cannot be resolved properly, which usually leads to unwanted spurious (nonphysical) oscillations in the numerical solution. The attenuation of these oscillations has been the subject of extensive research for several decades during which a huge number of so-called stabilized methods have been developed. The stabilizing effect can be often interpreted as the addition of some artificial diffusion to a standard (unstable) numerical scheme. On the one hand, this artificial diffusion should damp down the oscillations but, on the other hand, it should not smear the numerical solution so that the design of a proper stabilization is a very difficult task.

---

*Email address:* knobloch@karlin.mff.cuni.cz.

In the context of finite element methods, a very popular stabilization technique is the streamline upwind/Petrov–Galerkin (SUPG) method. This method was introduced by Brooks and Hughes [1] for advection–diffusion equations and incompressible Navier–Stokes equations. Later this technique has been applied to various other problems, e.g., coupled multidimensional advective–diffusive systems [6], first–order linear hyperbolic systems [9] or first–order hyperbolic systems of conservation laws [7]. Because of its structural simplicity, generality and the quality of numerical solutions, the SUPG method has attracted a considerable attention over the last two decades and many theoretical and computational results have been published. It is not the aim of this paper to provide a review of these results and we only refer to the monograph [13].

Like many other stabilized methods, the SUPG method contains a stabilization parameter for which a general ‘optimal’ choice is not known. Theoretical investigations of model problems only provide asymptotic behaviour of this parameter (with respect to the mesh width) and certain bounds for which the SUPG method is stable and leads to (quasi–)optimal convergence of the discrete solution. However, it has been reported many times that the choice of the stabilization parameter inside these bounds may dramatically influence the accuracy of the discrete solution. The aim of this paper is to describe a new way how the SUPG stabilization parameter can be defined.

For simplicity, we shall confine ourselves to a steady scalar convection–diffusion equation

$$-\varepsilon \Delta u + \mathbf{b} \cdot \nabla u = f \quad \text{in } \Omega. \quad (1)$$

We assume that  $\Omega$  is a bounded domain in  $\mathbb{R}^2$  with a polygonal boundary  $\partial\Omega$ ,  $\varepsilon > 0$  is the constant diffusivity,  $\mathbf{b}$  is a given convective field, and  $f$  is an outer source of  $u$ . The equation (1) has to be equipped with suitable boundary conditions on  $\partial\Omega$  which will be specified later. In the convection–dominated case  $\varepsilon \ll |\mathbf{b}|$ , the solution  $u$  typically contains interior and boundary layers (which depend on the choice of the boundary conditions). These layers can be divided into characteristic (interior and boundary) layers and outflow boundary layers, see [13].

The SUPG method produces accurate and oscillation–free solutions in regions where no abrupt changes in the solution of (1) occur but it does not preclude spurious oscillations (overshooting and undershooting) localized in narrow regions along sharp layers. Therefore, various, often nonlinear, terms introducing additional artificial diffusion in the neighborhood of layers have been proposed to be added to the SUPG formulation, see the recent review paper [8]. Such techniques are often called discontinuity–capturing methods, shock–capturing methods or spurious oscillations at layers diminishing (SOLD) methods.

Numerical tests in [8] revealed that the SOLD methods significantly improve the quality of a SUPG solution only if the SUPG method adds enough artificial diffusion in the streamline direction. This shows the necessity to reconsider the definition of the SUPG stabilization parameter. We shall confine ourselves to outflow boundary layers where a careful choice of the SUPG parameter can provide a fairly satisfactory approximation of the solution  $u$ . On the other hand, the choice of the stabilization parameter at characteristic layers has only a limited influence on the spurious oscillations appearing in these regions (cf., e.g., [11]). Indeed, characteristic layers follow the streamlines and the SUPG method contains no mechanism for stabilization in the direction perpendicular to streamlines where spurious oscillations occur. Therefore, an oscillation-free SUPG approximation of a characteristic layer can be obtained only by introducing an additional crosswind diffusion [8] or by using a layer-adapted mesh, see, e.g., [12].

The paper is organized in the following way. Sections 2 and 3 are devoted to the formulation of the SUPG method in one and two dimensions, respectively, and to a brief discussion of the optimal choice of the stabilization parameter. Then, in Section 4, the SUPG method is applied to a two-dimensional model problem and the insufficiency of the present approaches to the choice of the stabilization parameter is demonstrated. Based on the observations from Section 4, a new definition of the SUPG stabilization parameter at outflow boundary layers is derived in Section 5. Numerical results in Section 6 show the advantages of the new approach and the paper is closed by conclusions in Section 7. Throughout the paper, we use the standard notations  $P_1(\Omega)$ ,  $Q_1(\Omega)$ ,  $L^2(\Omega)$ ,  $H^1(\Omega) = W^{1,2}(\Omega)$ , etc. for the usual function spaces, see, e.g., Ciarlet [4]. For a vector  $\mathbf{a} \in \mathbb{R}^2$ , we denote by  $|\mathbf{a}|$  its Euclidean norm.

## 2 The SUPG method in one dimension

Let us consider the equation (1) in the one-dimensional case with homogeneous Dirichlet boundary conditions and  $\Omega = (0, 1)$ :

$$-\varepsilon u'' + b u' = f \quad \text{in } (0, 1), \quad u(0) = u(1) = 0. \quad (2)$$

For simplicity, let  $b$  and  $f$  be constants,  $b \neq 0$ . Then, denoting

$$\alpha = \frac{f}{b}, \quad \beta = \frac{b}{\varepsilon},$$

we have

$$u(x) = \alpha x - \alpha \frac{e^{-\beta(1-x)} - e^{-\beta}}{1 - e^{-\beta}}, \quad x \in [0, 1].$$

Thus, if  $\varepsilon \ll |b|$ , the solution  $u$  contains a boundary layer. Precisely, if  $b > 0$ , we see that  $u(x) \approx \alpha x$  on most of  $[0, 1)$  and a boundary layer occurs at  $x = 1$ .

Similarly, if  $b < 0$ , we have  $u(x) \approx \alpha(x - 1)$  on most of  $(0, 1]$  and a boundary layer occurs at  $x = 0$ .

Let  $N$  be a positive integer and let us set  $h = 1/N$  and define the nodes  $x_i = ih$ ,  $i = 0, 1, \dots, N$ . We introduce the finite element space

$$V_h = \{v \in C([0, 1]) ; v|_{[x_{i-1}, x_i]} \in P_1([x_{i-1}, x_i]), i = 1, \dots, N, \\ v(0) = v(1) = 0\}$$

consisting of continuous piecewise linear functions. Then the SUPG method for approximating the solution of (2) reads: Find  $u_h \in V_h$  such that

$$\varepsilon (u'_h, v'_h) + (b u'_h, v_h + \tau b v'_h) = (f, v_h + \tau b v'_h) \quad \forall v_h \in V_h, \quad (3)$$

where  $(\cdot, \cdot)$  denotes the inner product in  $L^2(0, 1)$  and  $\tau$  is a nonnegative stabilization parameter. This problem has a unique solution which is determined by the values  $u_i \equiv u_h(x_i)$ ,  $i = 0, \dots, N$ . If  $\tau$  is constant in  $(0, 1)$ , then (3) can be equivalently written in the form

$$-(\varepsilon + \tau b^2 + \frac{1}{2} b h) u_{i-1} + 2(\varepsilon + \tau b^2) u_i - (\varepsilon + \tau b^2 - \frac{1}{2} b h) u_{i+1} = f h^2, \quad (4)$$

where  $i = 1, \dots, N - 1$ .

It is well known that the parameter  $\tau$  can be chosen in such a way that the solution of (3) is nodally exact [3]. Indeed, setting

$$\tau = \frac{h}{2|b|} \left( \coth Pe - \frac{1}{Pe} \right) \quad \text{with} \quad Pe = \frac{|b| h}{2\varepsilon}, \quad (5)$$

it is easy to verify that  $u_i = u(x_i)$ ,  $i = 0, \dots, N$ . The quantity  $Pe$  is the local Péclet number which determines whether the problem is locally (i.e., within a particular subinterval) convection dominated or diffusion dominated.

If  $\mathbf{b}$  or  $f$  in (2) are not constant, then  $\tau$  defined by (5) generally does not lead to a nodally exact discrete solution. Nevertheless, the discrete solution is significantly better than the wildly oscillating solution of the standard Galerkin discretization (defined by (3) with  $\tau = 0$ ).

If the space  $V_h$  is constructed using higher-order polynomials, it is much more difficult to choose the parameter  $\tau$  in an appropriate way. For example, defining  $V_h$  using continuous piecewise quadratic functions, it was showed in [5] that a nodally exact discrete solution can be obtained only if a different formula is used for each of the two types of shape functions. This is, of course, not very convenient, particularly because an extension to the multidimensional case is rather complicated. Nevertheless, according to the considerations in [5] and various numerical experiments, a good choice seems to be to simply take half the value of  $\tau$  from (5).

### 3 The SUPG method in two dimensions

Let  $\mathcal{T}_h$  be a triangulation of the domain  $\Omega$  consisting of a finite number of open elements  $K$ . For simplicity, we shall assume that all elements of  $\mathcal{T}_h$  are either triangles or rectangles. Further, we assume that  $\bar{\Omega} = \bigcup_{K \in \mathcal{T}_h} \bar{K}$  and that the closures of any two different elements of  $\mathcal{T}_h$  are either disjoint or possess either a common vertex or a common edge.

We define the finite element space

$$W_h = \{v \in H^1(\Omega); v|_K \in R(K) \quad \forall K \in \mathcal{T}_h\},$$

where  $R(K) = P_1(K)$  if  $K$  is a triangle and  $R(K) = Q_1(K)$  if  $K$  is a rectangle. Further, we introduce a test function space  $V_h \subset W_h$  taking into account the boundary conditions prescribed for the solution of (1). For example, denoting by  $\partial\Omega^D$  and  $\partial\Omega^N$  disjoint subsets of  $\partial\Omega$  satisfying  $\overline{\partial\Omega^D} \cup \overline{\partial\Omega^N} = \partial\Omega$ , by  $\mathbf{n}$  the outward unit normal vector to  $\partial\Omega$  and by  $u_b$  a scalar function on  $\partial\Omega^D$ , the boundary conditions

$$u = u_b \quad \text{on } \partial\Omega^D, \quad \frac{\partial u}{\partial \mathbf{n}} = 0 \quad \text{on } \partial\Omega^N \quad (6)$$

lead to the space

$$V_h = \{v \in W_h; v = 0 \quad \text{on } \partial\Omega^D\}.$$

Of course, the triangulation  $\mathcal{T}_h$  should be defined in such a way that any boundary edge is a subset of  $\overline{\partial\Omega^D}$  or  $\overline{\partial\Omega^N}$ .

Denoting by  $u_{bh} \in W_h$  a function whose trace approximates the boundary condition  $u_b$ , the SUPG method for the convection–diffusion equation (1) equipped with the boundary conditions (6) reads:

Find  $u_h \in W_h$  such that  $u_h - u_{bh} \in V_h$  and

$$\varepsilon (\nabla u_h, \nabla v_h) + (\mathbf{b} \cdot \nabla u_h, v_h + \tau \mathbf{b} \cdot \nabla v_h) = (f, v_h + \tau \mathbf{b} \cdot \nabla v_h) \quad \forall v_h \in V_h, \quad (7)$$

where  $(\cdot, \cdot)$  denotes the inner product in  $L^2(\Omega)$  or  $L^2(\Omega)^2$  and  $\tau$  is a nonnegative stabilization parameter.

The choice of  $\tau$  significantly influences the quality of the discrete solution and therefore it has been a subject of an extensive research over the last three decades, see, e.g., the review in the recent paper [8]. Nevertheless, the definitions of  $\tau$  mostly rely on heuristic arguments and a general ‘optimal’ way of choosing  $\tau$  is still not known. Often, by analogy with the one–dimensional

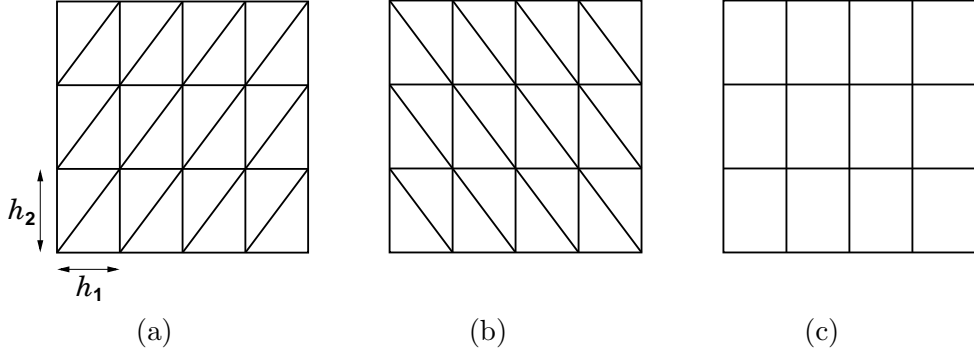


Fig. 1. Types of triangulations considered in Section 4.

formula (5), the parameter  $\tau$  is defined, on any element  $K \in \mathcal{T}_h$ , by

$$\tau|_K = \frac{h_K}{2|\mathbf{b}|} \left( \coth Pe_K - \frac{1}{Pe_K} \right) \quad \text{with} \quad Pe_K = \frac{|\mathbf{b}| h_K}{2\varepsilon}, \quad (8)$$

where  $h_K$  is the element diameter in the direction of the convection vector  $\mathbf{b}$ . Various justifications of this formula can be found in [8] (see also the next section). Note that, generally, the parameters  $h_K$ ,  $Pe_K$  and  $\tau|_K$  are functions of the points  $\mathbf{x} \in K$ .

#### 4 Application of the SUPG method to a model problem

Let  $\Omega = (0, 1)^2$  and let us consider the equation (1) with constant data  $f$  and  $\mathbf{b} \equiv (b_1, b_2)$  satisfying  $b_1 \neq 0$  and with the following boundary conditions:

$$u(0, y) = u(1, y) = 0 \quad \forall y \in (0, 1), \quad (9)$$

$$u(x, 0) = u(x, 1), \quad \frac{\partial u}{\partial y}(x, 0) = \frac{\partial u}{\partial y}(x, 1) \quad \forall x \in (0, 1). \quad (10)$$

This problem has a unique solution. Moreover, the solution is independent of  $y$  and satisfies (2) with  $b = b_1$ .

First, we shall confine ourselves to the three types of triangulations depicted in Fig. 1. The nodes are equidistant in both the  $x$ - and  $y$ -directions and the corresponding mesh widths are denoted by  $h_1$  and  $h_2$ , respectively. The test function finite element space is

$$V_h = \{v \in W_h; \ v(0, y) = v(1, y) = 0 \ \forall y \in (0, 1), \\ v(x, 0) = v(x, 1) \ \forall x \in (0, 1)\}$$

and the SUPG solution of the considered problem is a function  $u_h \in V_h$  satisfying (7). Again, this discrete solution is uniquely determined and, if  $\tau$  is constant, it does not depend on the  $y$ -coordinate. For both the triangular and the rectangular triangulations, the discrete solution then satisfies the one-dimensional scheme (4) with  $b = b_1$  and  $h = h_1$ . Thus, in view of (5), an



optimal choice of the stabilization parameter  $\tau$  in (7) is

$$\tau = \frac{h_1}{2|b_1|} \left( \coth Pe - \frac{1}{Pe} \right) \quad \text{with} \quad Pe = \frac{|b_1| h_1}{2\varepsilon}. \quad (11)$$

In this case the SUPG solution is nodally exact.

In the triangular case, the optimal one-dimensional scheme can be recovered also for piecewise constant  $\tau$ . It suffices when  $\tau$  has the same value on elements whose barycentres have the same  $x$ -coordinate and when, for any two elements  $K, K'$  sharing a ‘diagonal’ edge, we have

$$\frac{1}{2}(\tau|_K + \tau|_{K'}) = \frac{h_1}{2|b_1|} \left( \coth Pe - \frac{1}{Pe} \right) \quad \text{with} \quad Pe = \frac{|b_1| h_1}{2\varepsilon}. \quad (12)$$

Then the SUPG solution again is nodally exact.

If the convection vector  $\mathbf{b}$  points in the  $x$ -direction (i.e.,  $b_2 = 0$ ), then  $h_K = h_1$  and  $|\mathbf{b}| = |b_1|$  so that the formula (8) provides the optimal value of  $\tau$  determined by (11). This may be viewed as a justification of using (8) and, in particular, of defining  $h_K$  as the diameter of  $K$  in the direction of  $\mathbf{b}$  and not as the real diameter of  $K$ .

On the other hand, if  $b_2 \neq 0$ , the value provided by (8) is often smaller than the value of  $\tau$  given in (11), which leads to oscillations of  $u_h$ . Unfortunately, the above results also show that it is not possible to simply extend the one-dimensional considerations to the two-dimensional case by applying a formula for  $\tau$  of the type (8). Indeed, if we prescribe the homogeneous Dirichlet boundary conditions on the sides of  $\Omega$  parallel to the  $x$ -axis and the periodic boundary conditions on the sides of  $\Omega$  parallel to the  $y$ -axis, the optimal value of  $\tau$  will be given by

$$\tau = \frac{h_2}{2|b_2|} \left( \coth Pe - \frac{1}{Pe} \right) \quad \text{with} \quad Pe = \frac{|b_2| h_2}{2\varepsilon}.$$

However, an element  $K$  of the triangulation lying away from the boundary of  $\Omega$  does not have any information about its position in  $\Omega$  and the boundary conditions prescribed on  $\partial\Omega$  and hence, using only the information available on  $K$ , it is not possible to decide whether  $\tau$  on  $K$  should be defined by the value given in (11) or in (12).

Now, we shall investigate the following setting of the problem discussed in this section:

**Example 1** We consider the equation (1) in  $\Omega = (0, 1)^2$  with the boundary conditions (9) and (10) and with  $\varepsilon = 10^{-4}$ ,  $\mathbf{b} = (1, 0)$ , and  $f = 1$ .

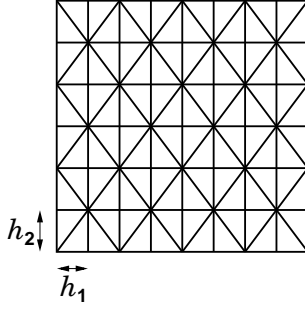


Fig. 2. Triangulation obtained by refining the triangulations from Fig. 1(a) and 1(b).

Let us solve Example 1 on a triangulation of the type depicted in Fig. 1(a) or 1(b). Then, as we know, the solution of the SUPG method with  $\tau$  defined by (8) is nodally exact. Often, a triangulation of a domain with a simple geometry is constructed by refining a coarse triangulation. If all triangles of the triangulations from Fig. 1(a) or 1(b) are divided into four equal triangles by connecting midpoints of edges, we obtain triangulations of the same type as in Fig. 1(a) or 1(b), respectively, and hence the corresponding SUPG solutions are again nodally exact. However, if we divide all triangles of the triangulations from Fig. 1(a) or 1(b) into four equal triangles by applying twice bisection, we obtain the triangulation depicted in Fig. 2 and the corresponding SUPG solution significantly differs from the nodally exact solution, see Fig. 3. Note that the triangulation in Fig. 2 contains the same type of triangles as the two triangulations in Figs. 1(a) and 1(b) and that also the orientation of the triangles with respect to the convection vector  $\mathbf{b}$  is the same as in Figs. 1(a) and 1(b). This again shows that the information available on a particular element of the triangulation is not sufficient for defining the stabilization parameter  $\tau$  in an optimal way and that the orientation of the neighbouring elements has to be taken into account.

The above examples of the behaviour of the SUPG method indicate the necessity to develop new strategies for defining the stabilization parameter  $\tau$ . A definition of  $\tau$  appropriate for elements lying at an outflow Dirichlet

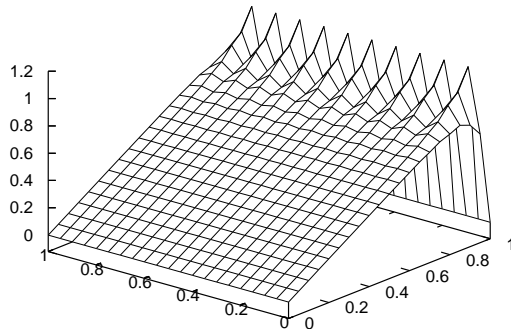


Fig. 3. Example 1, SUPG solution for  $\tau$  defined by (8) computed on the triangulation from Fig. 2 with  $h_1 = h_2 = 1/20$ .

boundary will be proposed in the next section.

**Remark 1** The periodic boundary conditions (10) considered in this section may seem artificial. However, the above discussion remains valid also for other types of boundary conditions. For example, if we prescribe homogeneous Dirichlet boundary conditions on the whole boundary of  $\Omega$ , choose  $\varepsilon \ll |\mathbf{b}| \approx f$  and use a rectangular domain  $\Omega$  with an appropriate ratio of the sides with respect to the direction of  $\mathbf{b}$ , then there will be a region in  $\Omega$  where both the exact and the discrete solution will behave very similarly as for the problem considered in this section.

**Remark 2** Let us consider the equation (1) in  $\Omega = (0, 1)^2$  with homogeneous Dirichlet boundary conditions,  $\varepsilon \ll 1$ ,  $\mathbf{b} = (1, 0)$ , and  $f = 1$ . Then the solution  $u$  possesses characteristic boundary layers at  $y = 0$  and  $y = 1$ . Using triangulations of the type considered in this section (being not extremely fine) and  $\tau$  defined by (8), the SUPG solution contains oscillations along  $y = 0$  and  $y = 1$  whereas the nodally exact solution satisfies  $u_h(x, y) \approx x$  at interior nodes. However, substituting the nodally exact solution into (7), we realize that, outside the outflow boundary layer, the SUPG terms cancel no matter how  $\tau$  is defined (in the rectangular case, this is true if  $\tau$  does not depend on  $x$ ). Thus, as we mentioned in the introduction, the SUPG method alone is not able to provide oscillation-free approximations to characteristic boundary layers unless layer-adapted meshes are used.

## 5 A new definition of the SUPG stabilization parameter

The favourable properties of the one-dimensional SUPG method (4) with  $\tau$  defined by (5) are due to the fact that the upwind character of the method increases with increasing Péclet number. Particularly, for  $Pe \gg 1$ , we have  $\tau \approx h/(2|b|)$  and the coefficient at the downwind node in (4) is

$$-(\varepsilon + \tau b^2 - \frac{1}{2}|b|h) \approx -\varepsilon.$$

Then the SUPG stabilization is basically equivalent to approximating the convective term by classical upwind differencing and the influence of the Dirichlet boundary condition at the outflow boundary node on the values of  $u_h$  at interior nodes is significantly suppressed.

In two dimensions, this property is generally lost, which leads to spurious oscillations like in Fig. 3. By analogy with the one-dimensional case, it is natural to ask whether  $\tau$  can be defined in such a way that, for  $\varepsilon \rightarrow 0$ , the difference scheme corresponding to (7) does not employ the outflow boundary values of  $u_h$ . Unfortunately, this is generally not possible. As an example, let us consider a triangulation of  $\Omega = (0, 1)^2$  of the type from Fig. 1(a) with  $h_1 = h_2 = h$  and let  $\varphi_j \in V_h$  be the standard basis function corresponding

to a boundary node  $\mathbf{x}_j$  lying on the right-hand side of  $\Omega$ . Let  $\varphi_i \in V_h$  be the standard basis function corresponding to the interior node  $\mathbf{x}_i$  connected with  $\mathbf{x}_j$  by a horizontal edge. Then, for  $\mathbf{b} = (2, 3)$ ,

$$(\mathbf{b} \cdot \nabla \varphi_j, \varphi_i + \tau \mathbf{b} \cdot \nabla \varphi_i) = \frac{h}{6} + \frac{2}{h^2} \int_{\text{supp } \varphi_i \cap \text{supp } \varphi_j} \tau \, d\mathbf{x} \quad (13)$$

and hence, for any choice of  $\tau$ , the value of  $u_h$  at  $\mathbf{x}_j$  contributes to the approximation of the convective term at  $\mathbf{x}_j$ .

Thus, let us at least investigate whether a suitable choice of  $\tau$  can remove the oscillations shown in Fig. 3. We denote the outflow Dirichlet boundary by  $\Gamma$ , i.e.,  $\Gamma = \{1\} \times [0, 1]$ , and we set

$$G_h = \bigcup_{K \in \mathcal{T}_h, \overline{K} \cap \Gamma \neq \emptyset} K.$$

Further, we denote by  $\varphi_1, \dots, \varphi_{M_h}$  all standard basis functions of  $V_h$  which satisfy

$$\text{supp } \varphi_i \cap G_h \neq \emptyset, \quad i = 1, \dots, M_h. \quad (14)$$

The nodally exact solution of Example 1 on the triangulation from Fig. 2 with  $h_1 = h_2 = 1/20$  satisfies  $u_h(x, y) \approx x$  in  $[0, 1 - h_1] \times [0, 1]$  and hence, neglecting the diffusion term, it satisfies (7) if and only if

$$\int_{G_h} v_h + \tau \mathbf{b} \cdot \nabla v_h \, d\mathbf{x} = 0 \quad \forall v_h \in V_h.$$

This can be equivalently written in the form

$$\int_{G_h} \varphi_i + \tau \mathbf{b} \cdot \nabla \varphi_i \, d\mathbf{x} = 0, \quad i = 1, \dots, M_h. \quad (15)$$

There are many possibilities how to fulfil these relations and the simplest one probably is to set

$$\tau|_K = \begin{cases} \frac{2h_1}{3} & \text{if } K \text{ has an edge on } \Gamma, \\ \frac{h_1}{3} & \text{otherwise} \end{cases} \quad \forall K \in \mathcal{T}_h, K \subset G_h. \quad (16)$$

On the remaining elements  $K \in \mathcal{T}_h$  we define  $\tau$  by (8). Then the SUPG solution is a very good approximation of the solution to Example 1 as Fig. 4 shows.

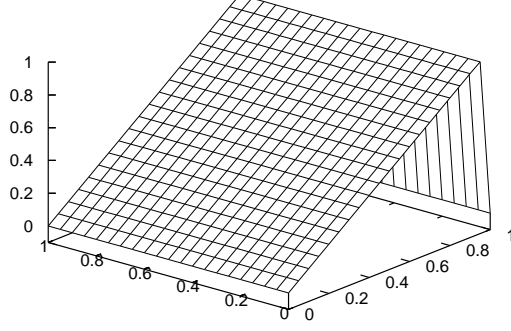


Fig. 4. Example 1, SUPG solution for  $\tau$  defined by (8) and (16) computed on the triangulation from Fig. 2 with  $h_1 = h_2 = 1/20$ .

The relations (15) used to define  $\tau$  were obtained thanks to the fact that the nodally exact solution of Example 1 satisfies

$$\mathbf{b} \cdot \nabla u_h - f \approx 0 \quad \text{in } \Omega \setminus \overline{\mathcal{G}_h}, \quad \mathbf{b} \cdot \nabla u_h - f = \text{const.} \quad \text{in } \overline{\mathcal{G}_h}. \quad (17)$$

For other data or boundary conditions, this will be usually not satisfied but it can be expected that the validity of (15) will diminish the spurious oscillations along an outflow boundary layer.

Let us now investigate whether (15) can be satisfied for a general polygonal domain  $\Omega$  and a triangulation  $\mathcal{T}_h$  consisting of triangles. Using the notation  $\partial\Omega^D$  for the part of  $\partial\Omega$  where Dirichlet boundary conditions are prescribed, we again introduce the outflow Dirichlet boundary

$$\Gamma = \overline{\{\mathbf{x} \in \partial\Omega^D; (\mathbf{b} \cdot \mathbf{n})(\mathbf{x}) > 0\}}.$$

For simplicity, we assume that  $\Gamma$  is connected and consists of whole boundary edges of  $\mathcal{T}_h$ . Like above, we set

$$\mathcal{G}_h = \bigcup_{K \in \mathcal{G}_h} K \quad \text{where} \quad \mathcal{G}_h = \{K \in \mathcal{T}_h; \overline{K} \cap \Gamma \neq \emptyset\}.$$

Further, we denote

$$\mathcal{G}_h^1 = \{K \in \mathcal{G}_h; K \text{ has only one vertex on } \Gamma\}, \quad \mathcal{G}_h^2 = \mathcal{G}_h \setminus \mathcal{G}_h^1.$$

For any vertex  $\mathbf{z} \in \Gamma$ , we denote by

$$\mathcal{G}_h^1(\mathbf{z}) = \{K \in \mathcal{G}_h^1; \mathbf{z} \in \overline{K}\}$$

the set of all elements possessing the vertex  $\mathbf{z}$  and no other vertex lying on  $\Gamma$ . For any  $K \in \mathcal{T}_h$ , we set

$$\mathbf{b}_K = \frac{1}{|K|} \int_K \mathbf{b} \, d\mathbf{x}.$$

If  $K \in \mathcal{G}_h^1$ , we assume that  $\mathbf{b}_K$  points from the vertex  $\overline{K} \cap \Gamma$  outwards  $\overline{K}$ . If  $K \in \mathcal{G}_h^2$  has exactly two vertices on  $\Gamma$ , we denote by  $\mathbf{n}_E$  the outward normal vector to the edge  $E$  connecting these two vertices and assume that  $\mathbf{b}_K \cdot \mathbf{n}_E > 0$ .

We again denote by  $\varphi_1, \dots, \varphi_{M_h}$  all standard basis functions of  $V_h$  satisfying (14). For  $i = 1, \dots, M_h$ , let  $\mathbf{x}_i$  be the vertex associated with the basis function  $\varphi_i$ , i.e.,  $\varphi_i(\mathbf{x}_i) = 1$  and  $\varphi_i(\mathbf{x}) = 0$  for any vertex  $\mathbf{x} \neq \mathbf{x}_i$ . We set

$$\begin{aligned} \mathcal{N}_h &= \{\mathbf{x}_1, \dots, \mathbf{x}_{M_h}\}, \\ \mathcal{N}_h^2 &= \{\mathbf{x} \in \mathcal{N}_h; \exists K \in \mathcal{G}_h^2 : \mathbf{x} \in \overline{K}\}, \quad \mathcal{N}_h^1 = \mathcal{N}_h \setminus \mathcal{N}_h^2. \end{aligned}$$

The example leading to (13) shows that it is generally not possible to fulfil (15) elementwise. Nevertheless, we can use the fact that each vertex  $\mathbf{x}_i$ ,  $i = 1, \dots, M_h$ , can be easily assigned to an element  $K \in \mathcal{G}_h$  (in an one-to-one way) such that  $\mathbf{b}_K \cdot \nabla \varphi_i|_K < 0$ . This follows from the following results.

**Lemma 1** *For any  $K \in \mathcal{G}_h^1$  satisfying  $\text{card}(\overline{K} \cap \mathcal{N}_h) = 2$ , there exists  $i \in \{1, \dots, M_h\}$  such that  $\mathbf{x}_i$  is a vertex of  $K$  and  $\mathbf{b}_K \cdot \nabla \varphi_i|_K < 0$ .*

*Proof.* Let us assume that the lemma is not true. Then there exist  $K \in \mathcal{G}_h^1$  and  $j, k \in \{1, \dots, M_h\}$  such that  $j \neq k$  and

$$\mathbf{x}_j, \mathbf{x}_k \in \overline{K}, \quad \mathbf{b}_K \cdot \nabla \varphi_j|_K \geq 0, \quad \mathbf{b}_K \cdot \nabla \varphi_k|_K \geq 0.$$

We denote by  $\mathbf{z}$  the remaining vertex of  $K$ . The vectors  $\nabla \varphi_j|_K$  and  $\nabla \varphi_k|_K$  are orthogonal to the edges  $\mathbf{z}, \mathbf{x}_k$  and  $\mathbf{z}, \mathbf{x}_j$ , respectively, and point into  $K$ . Consequently,  $\mathbf{b}_K$  points from the vertex  $\mathbf{z}$  into  $\overline{K}$ . This is not possible since  $\mathbf{z} \in \Gamma$ .  $\square$

**Lemma 2** *Let  $K \in \mathcal{G}_h^2$  satisfy  $\overline{K} \cap \mathcal{N}_h \neq \emptyset$  and let  $i \in \{1, \dots, M_h\}$  be such that  $\overline{K} \cap \mathcal{N}_h = \{\mathbf{x}_i\}$ . Then  $\mathbf{b}_K \cdot \nabla \varphi_i|_K < 0$ .*

*Proof.* Since the vector  $\nabla \varphi_i|_K$  is orthogonal to the edge  $E$  of  $K$  opposite the vertex  $\mathbf{x}_i$  and points into  $K$ , the lemma immediately follows from the assumptions on  $\mathbf{b}_K$ .  $\square$

**Lemma 3** *Let  $\mathbf{z} \in \Gamma$  be any vertex different from the end points of  $\Gamma$  and let  $\text{card} \mathcal{G}_h^1(\mathbf{z}) \geq 2$ . Let the edges of elements of  $\mathcal{G}_h^1(\mathbf{z})$  opposite  $\mathbf{z}$  form a connected curve, see Fig. 5. For simplicity, let us assume that there exist  $k, l \in \{1, \dots, M_h\}$  such that  $k \leq l$ ,*

$$\{\mathbf{x}_k, \dots, \mathbf{x}_l\} = \{\mathbf{x} \in \mathcal{N}_h; \exists K, K' \in \mathcal{G}_h^1(\mathbf{z}) : \mathbf{x} \in \overline{K} \cap \overline{K'}\}$$

and  $\text{card} \mathcal{G}_h^1(\mathbf{z}) = l - k + 2$ , see Fig. 5. Moreover, if  $k < l$ , we assume that, for  $i = k, \dots, l - 1$ , the vertices  $\mathbf{x}_i$  and  $\mathbf{x}_{i+1}$  are connected by an edge of

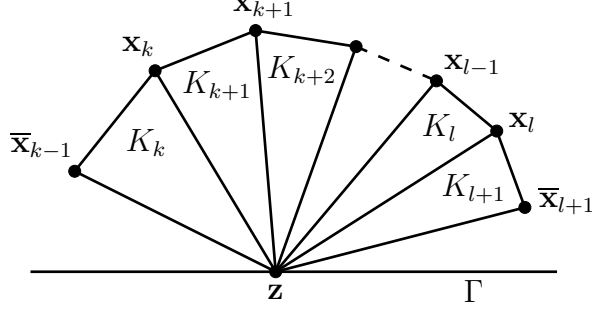


Fig. 5. Notation to Lemma 3.

the triangulation  $\mathcal{T}_h$ . Finally, we assume that  $\mathbf{b}$  is constant on the union of elements of  $\mathcal{G}_h^1(\mathbf{z})$ . We denote the elements of  $\mathcal{G}_h^1(\mathbf{z})$  by  $K_k, \dots, K_{l+1}$  in such a way that, for  $i = k, \dots, l$ , the elements  $K_i$  and  $K_{i+1}$  share the vertex  $\mathbf{x}_i$ . Further, we denote by  $\bar{\mathbf{x}}_{k-1}$  and  $\bar{\mathbf{x}}_{l+1}$  the remaining vertices of the elements  $K_k$  and  $K_{l+1}$ , respectively. Since these vertices may lie on  $\partial\Omega^D \setminus \Gamma$ , we denote the piecewise linear basis functions associated with these vertices by  $\bar{\varphi}_{k-1}$  and  $\bar{\varphi}_{l+1}$ , respectively. Then there exists  $j \in \{k, \dots, l+1\}$  such that

$$\begin{aligned} \mathbf{b} \cdot \nabla \varphi_i|_{K_i} &< 0, & \mathbf{b} \cdot \nabla \varphi_i|_{K_{i+1}} &\geq 0, & i &= k, \dots, j-2, \\ \mathbf{b} \cdot \nabla \varphi_i|_{K_i} &\geq 0, & \mathbf{b} \cdot \nabla \varphi_i|_{K_{i+1}} &< 0, & i &= j+1, \dots, l, \\ \mathbf{b} \cdot \nabla \bar{\varphi}_{k-1}|_{K_k} &\geq 0, & \mathbf{b} \cdot \nabla \varphi_{j-1}|_{K_{j-1}} &< 0 & \text{if } j > k, \\ \mathbf{b} \cdot \nabla \varphi_j|_{K_{j+1}} &< 0, & \mathbf{b} \cdot \nabla \bar{\varphi}_{l+1}|_{K_{l+1}} &\geq 0 & \text{if } j \leq l. \end{aligned}$$

*Proof.* For simplicity, we shall write  $\varphi_{k-1}$  and  $\varphi_{l+1}$  instead of  $\bar{\varphi}_{k-1}$  and  $\bar{\varphi}_{l+1}$ , respectively. The vector  $\nabla \varphi_k|_{K_k}$  is orthogonal to the edge  $\mathbf{z}, \bar{\mathbf{x}}_{k-1}$  and points into  $K_k$ . Similarly,  $\nabla \varphi_l|_{K_{l+1}}$  is a vector orthogonal to the edge  $\mathbf{z}, \bar{\mathbf{x}}_{l+1}$  which points into  $K_{l+1}$ . Since  $\mathbf{b}$  does not point from  $\mathbf{z}$  into  $\cup_{i=k}^{l+1} \bar{K}_i$ , we deduce that  $\mathbf{b} \cdot \nabla \varphi_k|_{K_k}$  or  $\mathbf{b} \cdot \nabla \varphi_l|_{K_{l+1}}$  is negative. Without loss of generality we may assume that  $\mathbf{b} \cdot \nabla \varphi_k|_{K_k} < 0$ . Then there exists  $j \in \{k, \dots, l+1\}$  such that

$$\mathbf{b} \cdot \nabla \varphi_i|_{K_i} < 0, \quad i = k, \dots, j,$$

and, if  $j \leq l$ ,

$$\mathbf{b} \cdot \nabla \varphi_{j+1}|_{K_{j+1}} \geq 0.$$

From the latter inequality, we derive analogously as at the beginning of the proof that

$$\mathbf{b} \cdot \nabla \varphi_i|_{K_{i+1}} < 0, \quad i = j, \dots, l.$$

Finally, since the vectors  $\nabla \varphi_{i-1}|_{K_i}$  and  $\nabla \varphi_{i+1}|_{K_{i+1}}$  have opposite directions for any  $i \in \{k, \dots, l\}$ , it follows from the above inequalities that

$$\begin{aligned} \mathbf{b} \cdot \nabla \varphi_i|_{K_{i+1}} &> 0, & i &= k-1, \dots, j-2, \\ \mathbf{b} \cdot \nabla \varphi_i|_{K_i} &> 0, & i &= j+2, \dots, l+1. \end{aligned} \quad \square$$

Lemmas 1–3 enable to introduce an algorithm for defining the SUPG parameter  $\tau$  at outflow Dirichlet boundaries. Since the relations (15) correspond to  $\varepsilon \rightarrow 0$ , we denote  $\tau$  satisfying (15) by  $\tau_0$ . Thus, we shall construct a piecewise constant function  $\tau_0$  on  $G_h$  satisfying

$$\int_{G_h} \varphi_i + \tau_0 \mathbf{b} \cdot \nabla \varphi_i \, d\mathbf{x} = 0, \quad i = 1, \dots, M_h. \quad (18)$$

Then, by analogy to (8), we define the parameter  $\tau$ , on any element  $K \in \mathcal{G}_h$ , by

$$\tau|_K = \tau_0|_K \left( \coth Pe_K - \frac{1}{Pe_K} \right) \quad \text{with} \quad Pe_K = \frac{|\mathbf{b}_K| h_K}{2\varepsilon}. \quad (19)$$

On elements  $K \in \mathcal{T}_h \setminus \mathcal{G}_h$ , we define  $\tau$  by (8) with  $\mathbf{b}$  replaced by  $\mathbf{b}_K$ .

Let us note that the definition of  $\tau_0$  is not important on elements which have all three vertices on the Dirichlet boundary since all functions from  $V_h$  vanish on these elements. Therefore, we shall not mention such elements in the following.

It is advantageous to start defining  $\tau_0$  on elements of  $\mathcal{G}_h^1$ . First, for any vertex  $\mathbf{z} \in \Gamma$  we construct the set  $\mathcal{G}_h^1(\mathbf{z})$ . If this set consists of one element  $K$ , the value of  $\tau_0$  on  $K$  can be defined arbitrarily. If  $\overline{K} \cap \mathcal{N}_h = \{\mathbf{x}_i\}$  for some  $i \in \{1, \dots, M_h\}$  and  $\mathbf{b}_K \cdot \nabla \varphi_i|_K \geq 0$ , we set  $\tau_0|_K = h_K/(2|\mathbf{b}_K|)$  like in (8). If  $\mathbf{b}_K \cdot \nabla \varphi_i|_K < 0$ , we can define  $\tau_0$  on  $K$  in such a way that

$$\int_K \varphi_i + \tau_0 \mathbf{b} \cdot \nabla \varphi_i \, d\mathbf{x} = 0.$$

However, the value of  $\tau_0$  determined from this relation tends to infinity if the vector  $\mathbf{b}_K$  approaches the direction of the edge of  $K$  opposite  $\mathbf{x}_i$ . Therefore, we introduce a positive parameter  $\alpha_{min}$  (e.g.,  $\alpha_{min} = 0.1$ ) and set

$$\tau_0|_K = \frac{1}{\max\{-3\mathbf{b}_K \cdot \nabla \varphi_i|_K, \alpha_{min} |\mathbf{b}_K|/h_K\}}. \quad (20)$$

If  $\overline{K} \cap \mathcal{N}_h = \{\mathbf{x}_i, \mathbf{x}_j\}$  for some  $i, j \in \{1, \dots, M_h\}$ ,  $i \neq j$ , we set

$$\tau_0|_K = -\frac{1}{3 \min\{\mathbf{b}_K \cdot \nabla \varphi_i|_K, \mathbf{b}_K \cdot \nabla \varphi_j|_K\}}. \quad (21)$$

This value of  $\tau_0$  is positive by Lemma 1 and, if  $\mathbf{z}$  is different from the end points of  $\Gamma$ , it is bounded by a constant depending on the minimal angle  $\theta$  in the elements of  $\mathcal{T}_h$ . Precisely, it can be shown that  $\tau_0|_K \leq h_K/(3 \min\{\frac{1}{2}, \sin^2 \theta\} |\mathbf{b}_K|)$ . The bound  $h_K/(3 \sin^2 \theta |\mathbf{b}_K|)$  corresponds to  $\mathbf{b}_K$  aligned with  $\Gamma$  so that the



values of  $\tau_0$  are smaller in practice. It is easy to see that in all three cases discussed above we have

$$\int_K \varphi_i + \tau_0 \mathbf{b} \cdot \nabla \varphi_i \, d\mathbf{x} \geq 0 \quad \forall \mathbf{x}_i \in \overline{K} \cap \mathcal{N}_h. \quad (22)$$

Now let  $\text{card } \mathcal{G}_h^1(\mathbf{z}) \geq 2$  and let  $\mathbf{z}$  be different from the end points of  $\Gamma$ . If necessary, we decompose  $\mathcal{G}_h^1(\mathbf{z})$  into several sets satisfying the assumptions of Lemma 3 or consisting of one element and we treat these sets separately. The treatment of single elements was discussed in the preceding paragraph and hence it suffices to consider the case when  $\mathcal{G}_h^1(\mathbf{z})$  satisfies the assumptions of Lemma 3. This lemma was formulated for a constant vector  $\mathbf{b}$  but if  $\mathbf{b}$  is non-constant, the assertion remains true provided that the triangulation  $\mathcal{T}_h$  is fine enough with respect to variations of  $\mathbf{b}$ . An alternative is to modify the discrete problem (7) in such a way that  $\mathbf{b}$  is replaced on the elements of  $\mathcal{G}_h^1(\mathbf{z})$  by its mean value. Thus, let us consider the notation of Lemma 3 and let  $j$  be the integer introduced in the assertion of this lemma. We define  $\tau_0$  on  $K_j$  in the same way as in the case  $\text{card } \mathcal{G}_h^1(\mathbf{z}) = 1$  discussed above. To fix ideas, let us assume that  $j \in \{k+1, \dots, l\}$ . Then we compute  $\tau_0$  on  $K_{j-1}$  and on  $K_{j+1}$  from the relations

$$\int_{K_{j-1} \cup K_j} \varphi_{j-1} + \tau_0 \mathbf{b} \cdot \nabla \varphi_{j-1} \, d\mathbf{x} = 0, \quad \int_{K_j \cup K_{j+1}} \varphi_j + \tau_0 \mathbf{b} \cdot \nabla \varphi_j \, d\mathbf{x} = 0. \quad (23)$$

Since  $\tau_0|_{K_j}$  is given by (21) with  $K = K_j$  and  $i = j-1$ , the inequality in (22) holds with  $K = K_j$  and  $i = j-1, j$ . Thus, it follows from Lemma 3 that the relations (23) determine both  $\tau_0|_{K_{j-1}}$  and  $\tau_0|_{K_{j+1}}$  uniquely and that both these values are positive. To determine  $\tau_0$  on the remaining elements of  $\mathcal{G}_h^1(\mathbf{z})$ , we require

$$\int_{K_i \cup K_{i+1}} \varphi_i + \tau_0 \mathbf{b} \cdot \nabla \varphi_i \, d\mathbf{x} = 0 \quad \text{for } i = k, \dots, j-2 \quad \text{and } i = j+1, \dots, l.$$

According to Lemma 3, the respective values of  $\tau_0$  can be easily computed and are positive. The cases  $j = k$  and  $j = l+1$  can be viewed as particular cases of the above procedure. Note also that, if  $\overline{\mathbf{x}}_{k-1} = \mathbf{x}_{k-1} \in \mathcal{N}_h$  or  $\overline{\mathbf{x}}_{l+1} = \mathbf{x}_{l+1} \in \mathcal{N}_h$ , we respectively have

$$\int_{K_k} \varphi_{k-1} + \tau_0 \mathbf{b} \cdot \nabla \varphi_{k-1} \, d\mathbf{x} \geq 0 \quad \text{or} \quad \int_{K_{l+1}} \varphi_{l+1} + \tau_0 \mathbf{b} \cdot \nabla \varphi_{l+1} \, d\mathbf{x} \geq 0. \quad (24)$$

Indeed, if  $\mathbf{b}_K \cdot \nabla \varphi_{k-1}|_{K_k} < 0$ , we have  $j = k$  in view of Lemma 3. As we explained above, the inequality in (22) is satisfied for  $K = K_j$  and  $i = j-1$  and hence the former inequality in (24) holds. The validity of the latter inequality in (24) follows analogously.

If  $\text{card } \mathcal{G}_h^1(\mathbf{z}) \geq 2$  and  $\mathbf{z}$  is an end point of  $\Gamma$ , we can often proceed in the same way as above. However, generally, it is not possible to guarantee the existence of  $\tau_0$  satisfying (18) for  $\mathbf{x}_i$  connected by an edge with this  $\mathbf{z}$ . On elements  $K \in \mathcal{G}_h^1(\mathbf{z})$  such that  $\mathbf{b}_K \cdot \nabla \varphi_i|_K \geq 0$  for any  $\mathbf{x}_i \in \overline{K} \cap \mathcal{N}_h$ , we set  $\tau_0|_K = h_K/(2|\mathbf{b}_K|)$  like in (8). If the above procedure leads to a negative value of  $\tau_0$  on some  $K \in \mathcal{G}_h^1(\mathbf{z})$ , we set  $\tau_0|_K = 0$ .

The above definition of  $\tau_0$  on elements of  $\mathcal{G}_h^1$  assures that (18) holds for any  $i \in \{1, \dots, M_h\}$  such that  $\mathbf{x}_i \in \mathcal{N}_h^1$ , possibly except some  $\mathbf{x}_i$  connected by an edge with an end point of  $\Gamma$ . Moreover, denoting for  $\mathbf{x}_i \in \mathcal{N}_h^2$

$$\mathcal{G}_h^{1,i} = \{K \in \mathcal{G}_h^1; \mathbf{x}_i \in \overline{K} \text{ and } \forall K' \in \mathcal{G}_h^2: \mathbf{x}_i \in \overline{K'} \Rightarrow \overline{K} \cap \overline{K'} = \mathbf{x}_i\},$$

we have (again possibly except some  $\mathbf{x}_i$  connected with an end point of  $\Gamma$ )

$$\sum_{K \in \mathcal{G}_h^{1,i}} \int_K \varphi_i + \tau_0 \mathbf{b} \cdot \nabla \varphi_i \, d\mathbf{x} = 0 \quad \forall \mathbf{x}_i \in \mathcal{N}_h^2.$$

Therefore, to satisfy (18), we may define  $\tau_0$  on any  $K \in \mathcal{G}_h^2$  with  $\overline{K} \cap \mathcal{N}_h = \{\mathbf{x}_i\}$  by

$$\sum_{\substack{K' \in \mathcal{G}_h^1 \cup \{K\}, \\ \text{meas}_1(\overline{K} \cap \overline{K'}) \neq 0}} \int_{K'} \varphi_i + \tau_0 \mathbf{b} \cdot \nabla \varphi_i \, d\mathbf{x} = 0. \quad (25)$$

Note that, in (25), we integrate over a set consisting of  $K$  and elements of  $\mathcal{G}_h^1$  sharing an edge with  $K$ . According to Lemma 2 and the inequalities (22) and (24), the value of  $\tau_0|_K$  is determined by (25) uniquely and is positive. This completes the definition of  $\tau_0$  on  $G_h$ . For clarity, we summarize the whole algorithm in Fig. 6.

**Remark 3** If we apply the above definition of  $\tau_0$  to Example 1 on the meshes from Figs. 1(a), 1(b) and 2, we obtain for  $\tau_0$  the values given in (16). Thus, in view of (12), the definition of  $\tau$  given in (19) leads to a nodally exact SUPG solution of Example 1 on meshes of the type depicted in Figs. 1(a) and 1(b).

**Remark 4** In view of Remark 2 it cannot be expected that the proposed approach will lead to satisfactory results if  $(\mathbf{b} \cdot \mathbf{n})/|\mathbf{b}| \rightarrow 0$  on  $\Gamma$ . This can be also deduced from the fact that, in this case, the value of  $\tau_0$  determined from (25) tends to infinity. The algorithm may also fail if the triangulation contains an element  $K \in \mathcal{G}_h^2$  of the type depicted in Fig. 7. Then the assumption  $\mathbf{b}_K \cdot \mathbf{n}_E > 0$  is typically not satisfied. The simplest remedy is to bisect the elements  $K, K'$  sharing the edge  $E$ . Note also that the triangulation should be constructed in such a way that the part of the boundary of the strip  $\overline{G}_h$  lying in  $\Omega$  copies the outflow boundary  $\Gamma$ . This helps to approximately satisfy the second relation in (17).

```

for  $K \in \mathcal{T}_h \setminus \mathcal{G}_h$  do
   $\tau_0|_K := h_K/(2|\mathbf{b}_K|)$ 
enddo
for vertices  $\mathbf{z} \in \Gamma$  do
  if  $\mathcal{G}_h^1(\mathbf{z}) = \{K\}$  then
    if  $\overline{K} \cap \mathcal{N}_h = \{\mathbf{x}_i\}$  then
      if  $\mathbf{b}_K \cdot \nabla \varphi_i|_K \geq 0$  then
         $\tau_0|_K := h_K/(2|\mathbf{b}_K|)$ 
      else
        use (20)
      endif
    else
      use (21)
    endif
  else
    decompose  $\mathcal{G}_h^1(\mathbf{z})$  into subsets satisfying the assumptions
    of Lemma 3 or consisting of one element
    if subset =  $\{K\}$  then
      define  $\tau_0|_K$  as for  $\mathcal{G}_h^1(\mathbf{z}) = \{K\}$ 
    else
      find  $j$  from Lemma 3 and define  $\tau_0|_{K_j}$  as for  $\mathcal{G}_h^1(\mathbf{z}) = \{K\}$ 
      for  $i \in \{k, \dots, l\}$  successively determine  $\tau_0$  to satisfy
        
$$\int_{K_i \cup K_{i+1}} \varphi_i + \tau_0 \mathbf{b} \cdot \nabla \varphi_i \, d\mathbf{x} = 0$$

      endif
    endif
  endif
enddo
for  $K \in \mathcal{G}_h^2$  do
  determine  $\tau_0|_K$  from (25)
enddo
for  $K \in \mathcal{T}_h$  do
  compute  $\tau|_K$  from (19)
enddo
REMARKS:
if  $K \in \mathcal{G}_h$  and  $\mathbf{b}_K \cdot \nabla \varphi_i|_K \geq 0 \, \forall \mathbf{x}_i \in \overline{K} \cap \mathcal{N}_h$  then
  do not use the above procedure and set  $\tau_0|_K := h_K/(2|\mathbf{b}_K|)$ 
after computing any new  $\tau_0|_K$  set
 $\tau_0|_K := \min\{\max\{\tau_0|_K, 0\}, h_K/(\alpha_{min}|\mathbf{b}_K|)\}$ 

```

Fig. 6. New definition of the SUPG parameter.

**Remark 5** For simple model problems, a piecewise constant function  $\tau_0$  such that (18) holds can be defined also in the quadrilateral case. However, in general, the existence of a nonnegative piecewise constant  $\tau_0$  satisfying (18) cannot be guaranteed. A remedy could be to use non-constant  $\tau_0$  on some

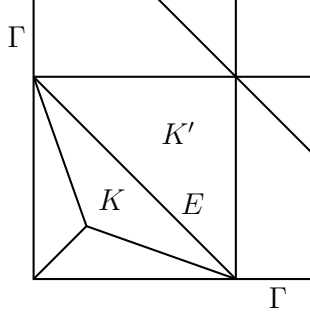


Fig. 7. Element  $K$  not satisfying the assumption  $\mathbf{b}_K \cdot \mathbf{n}_E > 0$ .

elements but this is not very convenient from the practical point of view. A further drawback of the quadrilateral case is that the definition of  $\tau_0$  is nonlocal. Therefore, it is advantageous to divide the quadrilaterals intersecting  $\Gamma$  into triangles and to use continuous piecewise linear functions in  $\overline{G_h}$  together with  $\tau_0$  defined by the algorithm in Fig. 6.

## 6 Numerical results

In this section we present some of our numerical results illustrating the properties of the approach proposed in the preceding section. We start with the following very simple model problem.

**Example 2** We consider the equation (1) and the boundary conditions (6) with  $\Omega = (0, 1)^2$ ,  $\partial\Omega^D = \partial\Omega$ ,  $\partial\Omega^N = \emptyset$ ,  $\varepsilon = 10^{-7}$ ,  $\mathbf{b} = (\cos(\pi/3), -\sin(\pi/3))$ ,  $f = 0$ , and

$$u_b(x, y) = \begin{cases} 0 & \text{for } x = 1 \text{ or } y = 0, \\ 1 & \text{else.} \end{cases}$$

We use a triangulation of the type from Fig. 1(a) with  $h_1 = h_2 = 1/20 \equiv h$ . The SUPG solution with  $\tau$  defined by (8), see Fig. 8(a), contains large spurious oscillations along both outflow boundary layers. On the other hand, if we define  $\tau$  by the algorithm in Fig. 6, we obtain a nodally exact solution, see Fig. 8(b).

We have already seen that there are usually many possibilities how to define a piecewise constant function  $\tau_0$  satisfying (18). Particularly, in the present example, we can use  $\tau_0$  which is constant for  $x < 1 - 2h$  and for  $y > 2h$ . Then  $\tau_0 = \frac{1}{2}h/|b_2| = h/\sqrt{3}$  in the former case and  $\tau_0 = \frac{1}{2}h/b_1 = h$  in the latter case. These values can also be obtained by the approach of Madden and Stynes [11] who adjusted the SUPG parameter in boundary layer regions in such a way that the artificial diffusion added by the SUPG method in the normal direction to an outflow boundary equals to the optimal value known from the one-dimensional case. Consequently, the approach of Madden and Stynes leads to

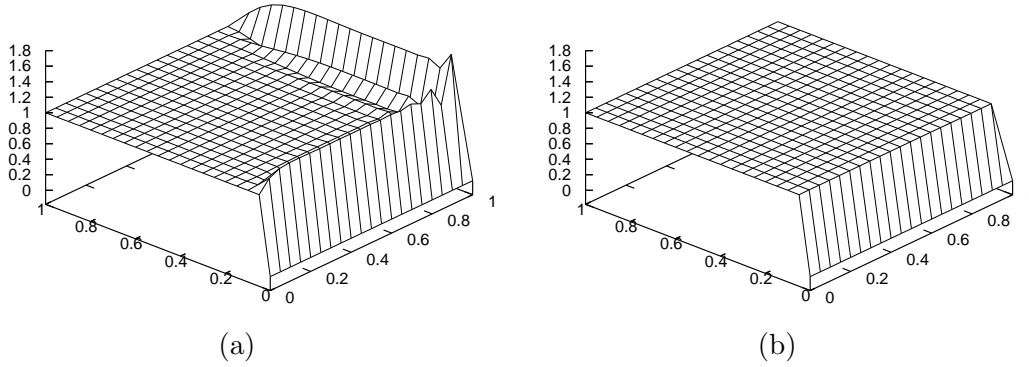


Fig. 8. Example 2, SUPG solutions computed on the triangulation from Fig. 1(a) with  $h_1 = h_2 = 1/20$ : (a)  $\tau$  defined by (8) (b)  $\tau$  defined by Fig. 6.

a discrete solution which is nodally exact except a small neighbourhood of the corner  $(1, 0)$ .

If we use a triangulation which is irregular along the outflow boundary, simple approaches like the one of Madden and Stynes typically do not work properly, which can also be deduced from the discussion in Section 4. As an example, let us consider the triangulation from Fig. 9(a) so that now  $h = 1/10$  in the normal direction to the boundary. Fig. 10(a) shows that the approach of Madden and Stynes does not give a satisfactory solution, which is due to the fact that the irregular triangulation does not allow to locally reduce the problem to the one-dimensional case. Nevertheless, the solution in Fig. 10(a) is much better than for  $\tau$  defined by (8). The discrete solution corresponding to  $\tau$  defined by the algorithm in Fig. 6 is still nodally exact, see Fig. 10(b). Let us mention that, in contrast to triangulations from Figs. 1 and 2, there is no rectangular grid associated with the triangulation from Fig. 9(a) which could be used for visualizing the computed solution. Therefore, in Fig. 10, we draw the graphs over all edges of the triangulation.

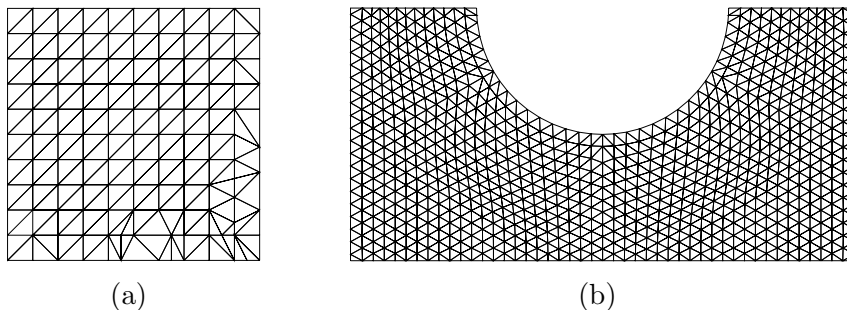


Fig. 9. Triangulations used in Section 6.

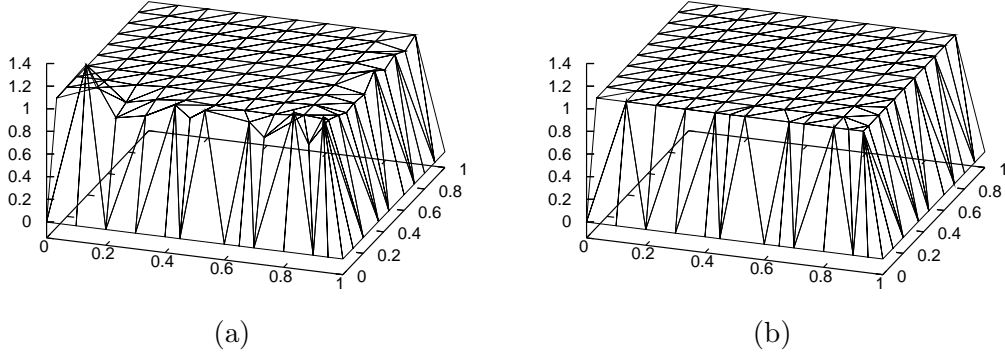


Fig. 10. Example 2, SUPG solutions computed on the triangulation from Fig. 9(a): (a)  $\tau$  defined according to Madden and Stynes [11] (b)  $\tau$  defined by Fig. 6.

A tuning of the SUPG parameter on elements intersecting an outflow boundary was also proposed by do Carmo and Alvarez [2]. However, on uniform triangulations like in Fig. 1, the parameter  $\tau$  would have the same value on all elements intersecting the outflow boundary, which does not enable to compute both boundary layers of Example 2 sharply.

On the triangulations considered above, the nodally exact solution  $u_h$  of Example 2 is constant in  $\Omega \setminus \overline{G_h}$  if  $\varepsilon \rightarrow 0$ . Moreover,  $\mathbf{b}$  and  $f$  are constant and the set  $\overline{G_h}$  can be decomposed into subsets on which  $u_h$  is linear and (18) holds. Thus, repeating the considerations from the beginning of Section 5, we can easily deduce that the nodally exact solution really solves (7) for  $\varepsilon \rightarrow 0$ . In the subsequent examples, such simple considerations will not be possible.

**Example 3** We consider the equation (1) and the boundary conditions (6) with  $\Omega = (0, 1)^2$ ,  $\partial\Omega^D = \partial\Omega$ ,  $\partial\Omega^N = \emptyset$ ,  $\varepsilon = 10^{-7}$ ,  $\mathbf{b} = (\cos(\pi/3), -\sin(\pi/3))$ ,  $f = 0$ , and

$$u_b(x, y) = \begin{cases} 0 & \text{for } x = 1 \text{ or } y = 0, \\ \sin \frac{(b_2 x - b_1 y) \pi}{b_2 - b_1} & \text{else.} \end{cases}$$

Note that now  $u_b$  is continuous. We shall consider the triangulation from Fig. 2 with  $h_1 = h_2 = 1/20$  on which the above-mentioned approach of Madden and Stynes does not lead to an oscillation-free solution. Fig. 11 shows that the SUPG solution obtained for  $\tau$  defined by (8) contains large spurious oscillations whereas a good approximation of the exact solution is obtained for  $\tau$  defined by the algorithm in Fig. 6.

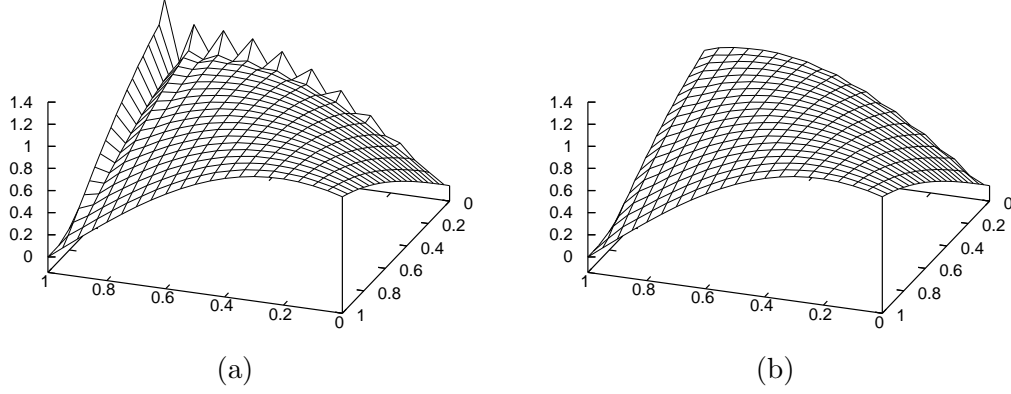


Fig. 11. Example 3, SUPG solutions computed on the triangulation from Fig. 2 with  $h_1 = h_2 = 1/20$ : (a)  $\tau$  defined by (8) (b)  $\tau$  defined by Fig. 6.

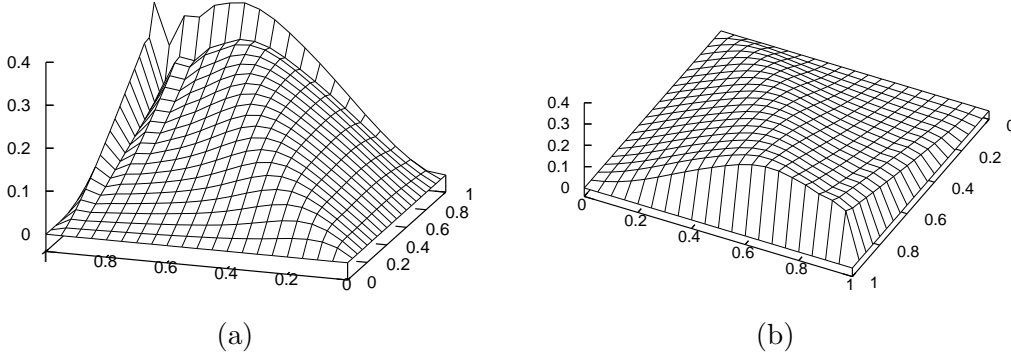


Fig. 12. Example 4, SUPG solutions computed on the triangulation from Fig. 1(b) with  $h_1 = h_2 = 1/20$ : (a)  $\tau$  defined by (8) (b)  $\tau$  defined by Fig. 6.

**Example 4** We consider the equation (1) and the boundary conditions (6) with  $\Omega = (0, 1)^2$ ,  $\partial\Omega^D = \partial\Omega$ ,  $\partial\Omega^N = \emptyset$ ,  $\varepsilon = 10^{-7}$ ,  $u_b = 0$ , and

$$\mathbf{b}(x, y) = (-y^3 + 2y + 1, 2x^2 - 3x + 2), \quad f(x, y) = \frac{\cos(x - y)}{1 + x + y}.$$

Using a triangulation of the type from Fig. 1(b) with  $h_1 = h_2 = 1/20$ , we obtain discrete solutions depicted in Fig. 12. The solution corresponding to  $\tau$  defined by (8) again contains large spurious oscillations. These oscillations disappear if  $\tau$  is defined by the algorithm in Fig. 6 although  $u$ ,  $\mathbf{b}$  and  $f$  are nonlinear. Note that we look from opposite sides at the graphs of the SUPG solutions in Fig. 12. To compute  $\tau$  from (8), we replaced  $\mathbf{b}|_K$  by its value at the barycentre of  $K$ . The terms from the discrete problem (7) were evaluated by means of quadrature formulas which were exact for piecewise linear  $\mathbf{b}$  and piecewise cubic  $f$ . A more precise integration does not lead to any visible difference in the computed solution.

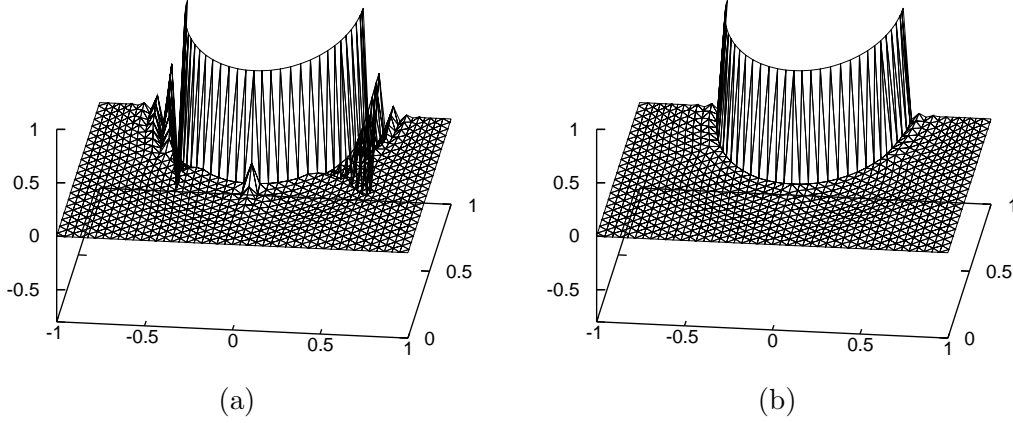


Fig. 13. Example 5, SUPG solutions computed on the triangulation from Fig. 9(b): (a)  $\tau$  defined by (8) (b)  $\tau$  defined by Fig. 6.

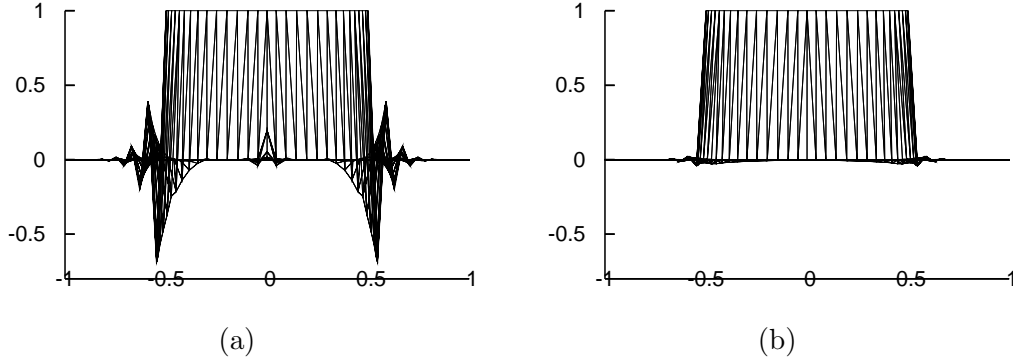


Fig. 14. Example 5, another view at the solutions from Fig. 13.

**Example 5** We consider the equation (1) and the boundary conditions (6) with

$$\Omega = \{(x, y) \in (-1, 1) \times (0, 1); x^2 + (y - 1)^2 > \frac{1}{4}\},$$

$$\partial\Omega^N = \{(-1, -\frac{1}{2}) \cup (\frac{1}{2}, 1)\} \times \{1\}, \quad \partial\Omega^D = \partial\Omega \setminus \partial\Omega^N,$$

$\varepsilon = 10^{-7}$ ,  $\mathbf{b} = (0, 1)$ ,  $f = 0$ , and

$$u_b(x, y) = \begin{cases} 1 & \text{for } x^2 + (y - 1)^2 = \frac{1}{4}, \\ 0 & \text{else.} \end{cases}$$

We use the triangulation depicted in Fig. 9(b). This example demonstrates that the algorithm in Fig. 6 can be successfully applied also if the outflow boundary is curved. The respective SUPG solution shown in Figs. 13(b) and 14(b) is not completely oscillation-free but the spurious oscillations are significantly smaller than for  $\tau$  defined by (8), see Figs. 13(a) and 14(a).



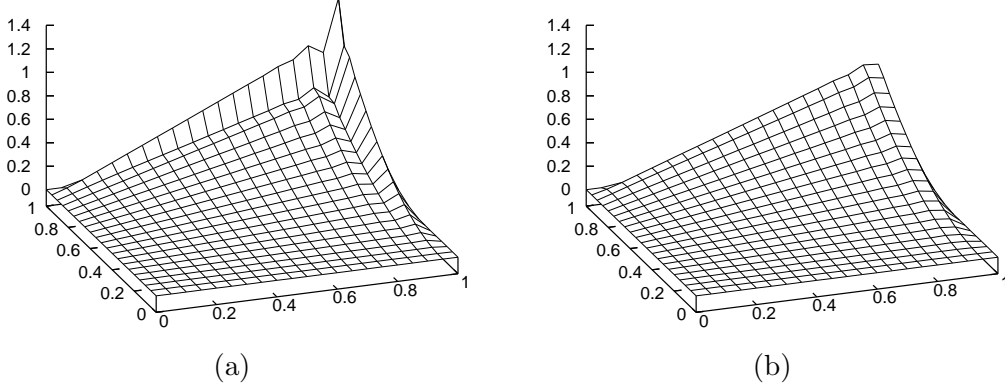


Fig. 15. Example 6, SUPG solutions computed on the triangulation from Fig. 1(b) with  $h_1 = h_2 = 1/20$ : (a)  $\tau$  defined by (8) (b)  $\tau$  defined by Fig. 6.

**Example 6** We consider the equation (1) and the boundary conditions (6) with  $\Omega = (0, 1)^2$ ,  $\partial\Omega^D = \partial\Omega$ ,  $\partial\Omega^N = \emptyset$ ,  $\varepsilon = 10^{-7}$ ,  $\mathbf{b} = (2, 3)$ , function  $f$  chosen in such a way that

$$u(x, y) = x y^2 - y^2 \exp\left(\frac{2(x-1)}{\varepsilon}\right) - x \exp\left(\frac{3(y-1)}{\varepsilon}\right) + \exp\left(\frac{2(x-1) + 3(y-1)}{\varepsilon}\right)$$

is the exact solution of (1), and with  $u_b = u|_{\partial\Omega}$ .

The function  $u$  contains two typical outflow boundary layers and hence this example represents a suitable tool for gauging the accuracy of numerical methods for the solution of convection–diffusion problems. In [10], we used this example for investigating the SUPG method with  $\tau$  defined by (8) on a sequence of triangulations of the type depicted in Fig. 1(b) with  $h_1 = h_2 \equiv h$ . The accuracy of the discrete solutions  $u_h$  was measured in various norms and it turned out that away the boundary layers the discrete solutions are rather accurate and converge to  $u$  with the usual optimal convergence rates. However, along the outflow boundary layers, the discrete solutions contain large spurious oscillations (see Fig. 15(a) for  $h = 1/20$ ) and the magnitude of these oscillations does not decrease for decreasing  $h$  as long as  $h \gg \varepsilon$ . This can be deduced from Table 1 where the second column contains values of the discrete maximum norm  $\|u - u_h\|_{0,\infty,h}$  defined as the maximum of the absolute values of the error  $u - u_h$  at vertices of the triangulation. We observe that  $\|u - u_h\|_{0,\infty,h}$  even slightly increases if the triangulations are refined.

Defining  $\tau$  by the algorithm in Fig. 6, the discrete solutions have the same accuracy away from layers as for  $\tau$  defined by (8), provided that the triangulations are sufficiently fine so that no spurious oscillations occur in the region on which norms of the errors of the discrete solutions are computed. However,

Table 1

Example 6, errors of SUPG solutions  $u_h$  computed for  $\tau$  defined by (8) or by Fig. 6 on triangulations from Fig. 1(b) with  $h_1 = h_2 \equiv h$

$\tau$	$\ u - u_h\ _{0,\infty,h}$		$\ u - u_h\ _{0,\infty,h}^*$	
	(8)	Fig. 6	(8)	Fig. 6
$h=5.000-2$	$5.08-1$	$5.48-2$	$9.37-3$	$2.45-3$
$h=2.500-2$	$5.70-1$	$2.90-2$	$2.32-4$	$6.28-5$
$h=1.250-2$	$6.02-1$	$1.49-2$	$7.06-6$	$6.97-6$
$h=6.250-3$	$6.18-1$	$7.54-3$	$1.74-6$	$1.74-6$
$h=3.125-3$	$6.27-1$	$3.80-3$	$4.35-7$	$4.35-7$
conv. order	-0.02	0.99	2.00	2.00

in contrast to discrete solutions obtained for  $\tau$  defined by (8), the discrete maximum norm  $\|u - u_h\|_{0,\infty,h}$  now linearly converges to zero for decreasing  $h$  also if  $h \gg \varepsilon$ , see the third column of Table 1. The values of  $\|u - u_h\|_{0,\infty,h}$  indicate that the large oscillations visible in Fig. 15(a) are not present in the SUPG solution obtained for  $\tau$  defined by Fig. 6, see also Fig. 15(b).

In Table 1 we also show values of the discrete maximum norm  $\|u - u_h\|_{0,\infty,h}^*$  defined as the maximum of  $|u - u_h|$  at vertices of the triangulation contained in the set  $[0, 0.8]^2$ . This set does not include a neighbourhood of the layers. As mentioned above, for both choices of  $\tau$ , the values of  $\|u - u_h\|_{0,\infty,h}^*$  are the same if  $h$  is sufficiently small and the convergence is of the optimal second order. The convergence orders in Table 1 are computed from the values for  $h = 6.25 \cdot 10^{-3}$  and  $h = 3.125 \cdot 10^{-3}$ .

## 7 Conclusions

In this paper we discussed the properties of the SUPG finite element method applied to the numerical solution of two-dimensional steady scalar convection-diffusion equations. We concentrated on the choice of the SUPG stabilization parameter  $\tau$  along outflow Dirichlet boundaries where the exact solution typically contains boundary layers. Most of the considerations were performed for conforming piecewise linear triangular finite elements. We demonstrated that an oscillation-free SUPG solution cannot be generally obtained if, on each triangle of the triangulation, the definition of  $\tau$  uses only the information available on the respective triangle. Therefore, we proposed a new approach for defining  $\tau$  on triangles intersecting an outflow Dirichlet boundary. On any such triangle  $K$ , the value  $\tau|_K$  generally depends not only on  $K$  and the convection vector  $\mathbf{b}|_K$  but also on the shape and orientation of triangles  $K'$  and convection vectors  $\mathbf{b}|_{K'}$  in a neighbourhood of  $K$ . Numerical results show a

significant reduction of spurious oscillations in discrete solutions in comparison to usual choices of  $\tau$  while accuracy away from layers is preserved. For simple model problems, even nodally exact solutions are obtained.

## Acknowledgments

This research is a part of the project MSM 0021620839 financed by MSMT and it was partly supported by the Grant Agency of the Academy of Sciences of the Czech Republic under the grant No. IAA100190505.

## References

- [1] A.N. Brooks, T.J.R. Hughes, Streamline upwind/Petrov–Galerkin formulations for convection dominated flows with particular emphasis on the incompressible Navier–Stokes equations, *Comput. Methods Appl. Mech. Engrg.* 32 (1982) 199–259.
- [2] E.G.D. do Carmo, G.B. Alvarez, A new upwind function in stabilized finite element formulations, using linear and quadratic elements for scalar convection–diffusion problems, *Comput. Methods Appl. Mech. Eng.* 193 (2004) 2383–2402.
- [3] I. Christie, D.F. Griffiths, A.R. Mitchell, O.C. Zienkiewicz, Finite element methods for second order differential equations with significant first derivatives, *Int. J. Numer. Methods Eng.* 10 (1976) 1389–1396.
- [4] P.G. Ciarlet, Basic error estimates for elliptic problems, in: P.G. Ciarlet, J.L. Lions (Eds.), *Handbook of Numerical Analysis*, v. 2 – Finite Element Methods (pt. 1), North–Holland, Amsterdam, 1991, pp. 17–351.
- [5] R. Codina, E. Oñate, M. Cervera, The intrinsic time for the streamline upwind/Petrov–Galerkin formulation using quadratic elements, *Comput. Methods Appl. Mech. Eng.* 94 (1992) 239–262.
- [6] T.J.R. Hughes, M. Mallet, A new finite element formulation for computational fluid dynamics: III. The generalized streamline operator for multidimensional advective–diffusive systems, *Comput. Methods Appl. Mech. Engrg.* 58 (1986) 305–328.
- [7] T.J.R. Hughes, T.E. Tezduyar, Finite element methods for first–order hyperbolic systems with particular emphasis on the compressible Euler equations, *Comput. Methods Appl. Mech. Engrg.* 45 (1984) 217–284.
- [8] V. John, P. Knobloch, On spurious oscillations at layers diminishing (SOLD) methods for convection–diffusion equations: Part I – A review, *Comput. Methods Appl. Mech. Engrg.* 196 (2007) 2197–2215.
- [9] C. Johnson, U. Nävert, J. Pitkäranta, Finite element methods for linear hyperbolic problems, *Comput. Methods Appl. Mech. Engrg.* 45 (1984) 285–312.

- [10] P. Knobloch, Improvements of the Mizukami–Hughes method for convection–diffusion equations, *Comput. Methods Appl. Mech. Engrg.* 196 (2006), 579–594.
- [11] N. Madden, M. Stynes, Linear enhancements of the streamline diffusion method for convection–diffusion problems, *Comput. Math. Appl.* 32 (1996) 29–42.
- [12] N. Madden, M. Stynes, Efficient generation of oriented meshes for solving convection–diffusion problems, *Int. J. Numer. Methods Engrg.* 40 (1997) 565–576.
- [13] H.–G. Roos, M. Stynes, L. Tobiska, *Numerical Methods for Singularly Perturbed Differential Equations. Convection–Diffusion and Flow problems*, 2nd ed., Springer–Verlag, Berlin, to appear.

## List of preprints released in this series

All preprints available on <http://www.karlin.mff.cuni.cz/ms-preprints/>  
E-mail contact to series administrator: [knm-prep@karlin.mff.cuni.cz](mailto:knm-prep@karlin.mff.cuni.cz)

- [MATH-MU-2007/1] Ondřej Kreml, Milan Pokorný: *A regularity criterion for the angular velocity component in* (04.01.2007)
- [MATH-MU-2007/2] Milan Pokorný, Piotr B. Mucha: *3D steady compressible Navier–Stokes equations* (04.01.2007)
- [MATH-MU-2007/3] Antonín Novotný, Milan Pokorný: *Stabilization to equilibria of compressible Navier–Stokes equations with infinite mass* (04.01.2007)
- [MATH-kma-2007/220] Eva Murtinova: *On (weakly) Whyburn spaces* (04.01.2007)
- [MATH-kma-2007/221] Petr Holický, C.E. Weil, Ludek Zajicek: *A note on the Darboux property of Frechet derivatives* (04.01.2007)
- [MATH-alg-2007/1] V. Repnitskii and J. Tma: *Intervals in subgroup lattices of countable locally finite groups* (10.01.2007)
- [MATH-alg-2007/2] D. Joščák and J. Tůma: *Multi-block Collisions in Hash functions based on 3C and 3C+ Enhancements of the Merkle-Damgard Construction* (10.01.2007)
- [MATH-alg-2007/3] J. Krajíček: *An exponential lower bound for a constraint propagation proof system based on ordered binary decision diagrams* (10.01.2007)
- [MATH-kma-2007/222] Josef Danecek, Oldrich John, Jana Stara: *Remarks on  $C^{1,\gamma}$  regularity of weak solutions to elliptic systems with BMO gradients* (16.01.2007)
- [MATH-kma-2007/223] Tomas Barta: *Delayed quasilinear evolution equations with application to heat flow* (16.01.2007)
- [MATH-alg-2007/4] V. Flaška, J. Ježek, T. Kepka and J. Kortelainen: *Transitive closures of binary relations I* (17.01.2007)
- [MATH-alg-2007/5] V. Flaška, J. Ježek, and T. Kepka: *Transitive closures of binary relations II* (17.01.2007)
- [MATH-alg-2007/6] J. Trlifaj: *Filtrations for the roots of Ext* (17.01.2007)
- [MATH-alg-2007/7] P. Csörgő, A. Drpal: *Loops that are conjugacy closed modulo the center* (01.02.2007)
- [MATH-alg-2007/8] J. Žemlička: *On self-small modules* (02.03.2007)
- [MATH-alg-2007/9] P. Csrg, A. Drpal and M. K. Kinyon: *Buchsteiner loops* (05.03.2007)
- [MATH-alg-2007/10] P. Csrg, A. Drpal: *Buchsteiner loops and conjugacy closedness* (05.03.2007)
- [MATH-kma-2007/224] Dalibor Prazak: *Exponential attractors for abstract parabolic systems with bounded delay* (06.03.2007)
- [MATH-kma-2007/225] Tomas Barta: *A generation theorem for hyperbolic equations with coefficients of bounded variation in time* (06.03.2007)
- [MATH-kma-2007/226] Eduard Feireisl, Dalibor Prazak: *A stabilizing effect of a high-frequency driving force on the motion of a viscous, compressible, and heat conducting fluid* (06.03.2007)
- [MATH-kma-2007/227] A. Aviles, Ondrej Kalenda: *Fiber orders and compact spaces of uncountable weight* (06.03.2007)

- [MATH-kma-2007/228] Andrea Cianchi, Ron Kerman, Lubos Pick: *Trace inequalities and rearrangements* (11.04.2007)
- [MATH-kma-2007/229] Miroslav Husek: *Urysohn universal space, its development and Hausdorff's approach* (11.04.2007)
- [MATH-kma-2007/230] Ondrej Kurka: *Reflexivity and sets of Frechet subdifferentiability* (11.04.2007)
- [MATH-kma-2007/231] Miroslav Posta: *On partial regularity of solutions to the quasilinear parabolic system up to the boundary* (11.04.2007)
- [MATH-knm-2007/1] V. Dolejsi, M. Feistauer, V. Kucera, V. Sobotikova: *An optimal  $L^\infty(L^2)$ -error estimate of the discontinuous Galerkin method for a nonlinear nonstationary convection-diffusion problem* (12.04.2007)
- [MATH-alg-2007/11] A. Drpal: *A nuclear construction of loops with small inner mapping groups* (13.04.2007)
- [MATH-kma-2007/232] Stanislav Hencl, Pekka Koskela, Jani Onninen: *Homeomorphisms of bounded variation* (16.04.2007)
- [MATH-kma-2007/233] Ondrej Kalenda: *On products with the unit interval* (16.04.2007)
- [MATH-kma-2007/234] Miroslav Bacak, Jiri Spurny: *Complementability of spaces of affine continuous functions on simplices* (21.04.2007)
- [MATH-kma-2007/235] Jaroslav Milota: *Invitation to mathematical control theory* (21.04.2007)
- [MATH-knm-2007/2] V. Dolejsi: *Analysis and application of IIPG method to quasilinear nonstationary convection-diffusion problems* (02.05.2007)
- [MATH-alg-2007/12] R. El Bashir, T. Kepka: *Congruence-simple semirings* (09.05.2007)
- [MATH-alg-2007/13] A.Drpal and P. Vojtchovsk: *Explicit constructions of loops with commuting inner mappings* (11.05.2007)
- [MATH-alg-2007/14] L. Angeleri Huegel, D. Herbera and J. Trlifaj: *Baer and Mittag-Leffler modules over tame hereditary algebras* (14.05.2007)
- [MATH-MU-2007/4] Eva B. Vedel Jensen, Jan Rataj: *A rotational integral formula for intrinsic volumes* (14.05.2007)
- [MATH-kma-2007/236] David Chodounsky, Eva Murtinova: *Internal normality and internal compactness* (15.05.2007)
- [MATH-kma-2007/237] Ondrej Kurka: *On Borel classes of sets of Frechet subdifferentiability* (15.05.2007)
- [MATH-alg-2007/15] J. Šároch and J. Šťovíček: *The countable telescope conjecture for module categories* (15.05.2007)
- [MATH-alg-2007/16] V.Kala, T.Kepka: *Notes on finitely generated ideal-simple commutative semirings* (15.05.2007)
- [MATH-alg-2007/17] S.Bazzoni and J. Šťovíček: *Sigma-cotorsion modules over valuation domains* (17.05.2007)

- [MATH-kma-2007/238] Jiri Spurny: *The Dirichlet problem for Baire-two functions on simplices* (22.06.2007)
- [MATH-kma-2007/239] Jiri Spurny: *Automatic boundedness of affine functions* (22.06.2007)
- [MATH-kma-2007/240] Jiri Spurny, Miroslav Zeleny: *Additive families of low Borel classes and Borel measurable selectors* (22.06.2007)
- [MATH-kma-2007/241] Petr Holicky, Ondrej Kalenda, Libor Vesely, Ludek Zajicek: *Quotients of continuous convex functions on non-reflexive Banach spaces* (22.06.2007)
- [MATH-kma-2007/242] Libor Vesely, Ludek Zajicek: *On compositions of d.c. functions and mappings* (22.06.2007)